RESEARCH ARTICLE

Time-Series Analysis of Surface-Water Quality in Xiong'an New Area, 2016–2019

Mingxiu Wang[1,2] · Yue Yao[2] · Qian Shen[2] · Hongjie Gao[3] · Junsheng Li[2] · Fangfang Zhang[2] · Qingshuang Wu[1]

Abstract

The Xiong'an New Area was established by the Chinese government on 1 April 2017 as a new district in the Hebei Province, and soon after its establishment, investigations on the waterbodies of the district began to initiate governance. In this study, data from 105 Sentinel-2 cloudless images for the period April 2016–September 2019 were analysed to understand the changes in the concentrations of chlorophyll-*a* and water turbidity in surface waterbodies of the Xiong'an New Area. The results suggest that (1) the water quality shows an overall improving trend owing to surface-water pollution control measures by the Chinese government in the region; (2) the turbidity of the surface waterbody declined gradually particularly after the spring of 2017; (3) the concentration of chlorophyll-*a* shows a weak decreasing trend, with a low value in spring and a high value in summer with a four-year average of 31.3 μg/L; and (4) by comparing the results of the water quality of two ponds inside and outside the Lake Baiyangdian and the overall water quality of Xiong'an New Area, the changes in turbidity and chlorophyll-*a* concentration during the study period were consistent.

Keywords Xiong'an New Area · Surface waterbody · Water quality · Time-series change

✉ Qian Shen
shenqian@radi.ac.cn

Mingxiu Wang
Mingxiuwang@ahnu.edu.cn

Yue Yao
yaoyue@aircas.ac.cn

Hongjie Gao
gaohj@craes.org.cn

Junsheng Li
lijs@radi.ac.cn

Fangfang Zhang
zhangff07@radi.ac.cn

Qingshuang Wu
wuqing@mail.ahnu.edu.cn

[1] Anhui Normal University, Wuhu 241000, China

[2] Key Laboratory of Digital Earth Science, Aerospace Information Research Institute, Chinese Academy of Sciences, Beijing 100049, China

[3] Chinese Research Academy of Environmental Sciences, Beijing 100012, China

Introduction

On 1 April 2017, the Central Committee of the Communist Party of China and the State Council established a new state-level district called the Xiong'an New Area in the Hebei Province. The surface water of the Xiong'an New Area is dominated by the Lake Baiyangdian (Liu et al. 2006; Su et al. 2011; Xu et al. 2012; Zhao et al. 2012; Li et al. 2017a, b; Wang et al. 2018; Song et al. 2018), and its distribution is relatively small and broken. The area has many sewage pits and ponds, which impair the construction of the Xiong'an New Area. Therefore, after the district was established, investigations on and treatments of these small waterbodies began. As of November 2018, a total of 810 polluted pools have been inspected in the three counties of the Xiong'an New Area (Zhao et al. 2020). The Chinese government has invested a lot of human and financial resources in governance, and there is an urgent need to evaluate the governance effects of the Chinese government.

Remote sensing has the advantages of large-scale applicability, high speed, and traceable history (Wei et al. 2020). The use of remote sensing for monitoring the

surface-water quality of the Xiong'an New Area can quickly and accurately reflect the effect of treatment on the sewage treatment ponds. Because the surface waterbodies in this area are relatively small and fragmented, it is necessary to select a satellite image with a high spatial resolution for monitoring them (Brezonik et al. 2005; Vincent et al. 2004). In addition, for sufficient time-monitoring frequency, it is necessary to select images with a high temporal resolution (Lambin et al. 1994). Therefore, in this study, we used the images obtained from the multispectral imager of the Sentinel-2 twin satellites. Satellites A and B can cover 13 spectral bands with spatial resolutions of 10, 20, and 60 m and widths of up to 290 km. One satellite has a revisit period of 10 days, and both satellites have a complementary revisit period of 5 days each (Drusch et al. 2012; Chen et al. 2017; Kutser et al. 2016; Liu et al. 2017; Toming et al. 2016). In addition, Sentinel-2 datasets include information from three bands (central wavelengths of 705, 740, and 783 nm) in the red edge range (Vanhellemont et al. 2019), which is more advantageous than other satellites in monitoring chlorophyll-a content in water.

To use the Sentinel-2 data for monitoring surface-water quality, the images must first be preprocessed, which involves atmospheric correction. Kuhn et al. (2019) performed comparisons among three atmospheric-correction methods, i.e. LaSRC, SeaDAS, and ACOLITE, and showed that in most cases, the three atmospheric-correction methods will produce the same order of magnitude of spectrum. However, for water applications, LaSRC is not as effective as SeaDAS and ACOLITE because the remote-sensing reflectivity produced by LaSRC is 36% higher than those of ACOLITE and SeaDAS. Caballero et al. (2018) analysed various satellite data using ACOLITE, Sen2cor, and QUAC and showed that although ACOLITE can be applied to Sentinel-2 images, it tends to mask some small and broken waterbodies, and the atmospheric-correction results cannot be obtained. Sola et al. (2018) compared four atmospheric-correction methods (Sen2cor, MAJA, Icor, and 6S) based on Sentinel-2 images and measured the obtained spectra. The results obtained from these methods did not differ significantly and showed high accuracy with an R^2 value of > 0.90. The root-mean-square error (RMSE) is less than 0.04 sr^{-1}. Warren et al. (2019) compared six kinds of atmospheric-correction algorithms (ACOLITE, C2RCC, Icor, l2gen, Polymer, and Sen2cor) available for Sentinel-2. The results show that Sen2cor has better accuracy. In summary, Sen2cor is a good atmospheric-correction method for Sentinel-2 data.

Many scholars, both domestically and internationally, have studied the remote-sensing retrieval of inland water-quality parameters (Chowdhury et al. 2014; Rostami et al. 2018). However, there are relatively few studies on the retrieval of water-quality parameters based on Sentinel-2 data. Based on the Sentinel-2 and Sentinel-3 satellites, Li et al. (2017a, b) solved the problem of unsuccessful retrieval of chlorophyll in some turbid waterbodies of Poyang Lake to a certain extent. Xu et al. (2019) proposed a spectral space-segmentation-guided ensemble method based on Sentinel-2 data and compared them with three separate empirical algorithms to better estimate the concentration of chlorophyll-a. Huovinen et al. (2019) studied the seasonal trends (long-term average) of the surface-water temperature, turbidity, and chlorophyll-a of Lake Panguipulli in central and southern Chile through Sentinel-2 and Landsat images. The verification of the measured data showed that the turbidity and chlorophyll-a concentration of the lake appeared low in summer.

Moreover, some scholars studied the evolution of the waterbody in the Xiong'an New Area and the changes in wetlands in Lake Baiyangdian. Song et al. (2018) analysed the detailed evolution of the flooded area in the Xiong'an New Area based on the long-sequence Landsat images from 1984 to 2016 including inter-annual, seasonal, and abrupt changes. The study has shown that the Lake Baiyangdian waterbody degradation is closely related to many aspects of human activities including dam construction, groundwater extraction, agricultural irrigation, tourism, and aquaculture. Zhu et al. (2019) analysed the spatial and temporal characteristics of changes in the wetlands of Lake Baiyangdian over the past 43 years based on 10 Landsat satellite remote-sensing images from 1975 to 2018 supplemented by Gaofen-2 (GF-2) satellite remote-sensing images of 2017–2018. There is still a lack of research on the water quality in the Xiong'an New Area.

Most retrieval studies have shown that the water-quality parameters are affected by the spatial resolution of the images, and most of them are aimed at large waterbodies such as lakes and reservoirs. Only few studies have been conducted on time-series changes of water quality of small and broken inland waterbodies. Therefore, in this study, the chlorophyll-a concentration and turbidity data of the surface waterbodies of the Xiong'an New Area from 2016 to 2019 were retrieved from higher-resolution Sentinel-2 data, and the time-series changes in water quality were statistically analysed.

Research Area and Data

Research Area and Measured Data

The Xiong'an New Area is located in Baoding City, Hebei Province, China. The planning samples cover three small counties, namely Xiong County, Rongcheng, and Anxin, and some surrounding areas in the Hebei Province with an

area of approximately 1563.31 km^2. The dominant surface waterbody in the new area is Lake Baiyangdian with some ponds and other waterbodies scattered outside the area of the lake. On 1 May 2019, a quasi-synchronous transit experiment was performed on remote-sensing data obtained from the Sentinel-2 satellites of the Xiong'an New Area. A dataset of 29 samples was obtained, which was used to establish a retrieval algorithm of chlorophyll-a concentration and water turbidity. On 5 October 2018, a synchronous transit experiment was performed on the remote-sensing data obtained from the Sentinel-2 satellites of the Xiong'an New Area, and a total of nine samples were obtained. Among them, the waterbody from which two samples were obtained was considerably small to be clearly identified on the image. Therefore, these two samples were eliminated, and finally the data from seven samples were used to test the retrieval algorithm of chlorophyll-a concentration and water turbidity. The location of the study area and the distribution of the experimental samples are shown in Fig. 1.

Screening of Remote-Sensing Image Data

This study uses Sentinel-2 data of the spring (April to May), summer (June–August), and autumn (September–October) of 2016, 2017, 2018, and 2019. The first frost day in the Xiong'an New Area is usually 19 October, and the frost normally lasts until 12 April; this was the basis for selecting non-icing data in this paper. In addition, images with less cloudiness were selected for the analyses. As the Xiong'an New Area is at the junction of three Sentinel-2 images, the Sentinel Application Platform (SNAP) recommended by the European Space Agency (ESA) must be used to mosaic the cloudless images taken on the same day, and hence, only less amount of data could meet the requirements. Finally, a total of 102 images of 34 phases were screened out. The specific image-selection schedule is shown in Table 1. The 2016–2018 Sentinel-2 data downloaded from ESA in this article are L1C-level data, and the 2019 Sentinel-2 data are L2A-level data. The L1C-level data are geometrically corrected orthophotos, and the L2A-level data are presented from L1C atmospherically corrected images.

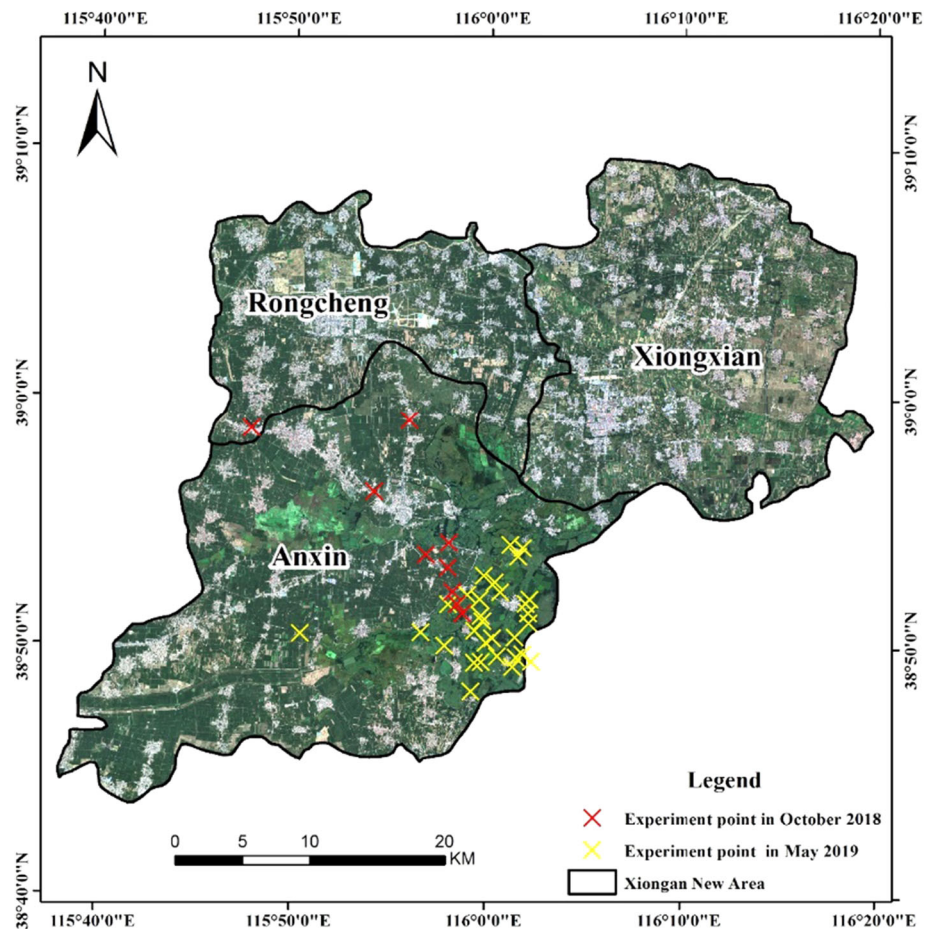**Fig. 1** Location of the study area and distribution of field samples

Table 1 Image-selection schedule

Year	Spring	Summer	Autumn
2016	13 April	12 June	20 September
	3 May	22 June	30 September
	13 May	31 August	10 October
2017	29 March	7 June	20 September
	18 April	27 June	5 October
	18 May	6 August	30 October
	28 May	–	–
2018	18 April	12 June	7 September
	28 April	–	5 October
	23 May	–	30 October
2019	13 May	12 July	25 September
	23 May	21 August	30 September
	28 May	31 August	–

Table 1 shows that when analysing temporal and spatial changes of water quality in each season, the pixel values of the same position of all the images in the season are averaged. The average image represents the water-quality status of that season; if there is only one phase in a season, it represents the water quality of that particular season by default.

Obtaining Measured Data

A field-SpecR3 portable ground spectrometer of the American ASD was used, and the water-spectrum measurement method proposed by NASA Marine Optical Specifications (Mueller et al. 2003) and Tang et al. (2004) was used to collect the remote-sensing reflectance of each sampling point. Furthermore, to better analyse the band characteristics of Sentinel-2 data and evaluate the effect of atmospheric correction, the equivalent reflectance measured on 5 October 2018 must be calculated to obtain the equivalent spectral reflectance corresponding to the Sentinel-2 band. The spectral equivalent can be calculated as

$$\rho = \frac{\int_{\lambda_{\min}}^{\lambda_{\max}} F_0(\lambda) \rho(\lambda) f(\lambda) d\lambda}{\int_{\lambda_{\min}}^{\lambda_{\max}} F_0(\lambda) f(\lambda) d\lambda} \tag{1}$$

where F_0 is the solar irradiance outside the atmosphere; $\rho(\lambda)$ is the reflectance at each wavelength on the ground, which is the reflectance spectrum measured on our ground; and $f(\lambda)$ is the spectral response function of each band of the remote sensor. The measured spectral reflectance and Sentinel-2 equivalent spectral reflectance are shown in Fig. 2.

Turbidity (NTU) was measured using the Orion AQ3010 turbidity meter (Thermo Scientific, USA). The hot ethanol

method was used to measure the concentration of chlorophyll-a in water. A GF/F glass fibre filter membrane with a pore size of 0.7 μm and diameter of 47 mm was used to filter the water samples collected in the field experiment. Then, the used folded filter membrane was put it in a test tube for freezing for 48 h. Later, it was taken out of the refrigerator and approximately 4 mL of hot ethanol was added to the test tube with the filter membrane and heated to 85 °C in a water bath for 4–6 h and the extract was filtered with another 0.7-μm membrane with a pore diameter of 25 mm and 90% ethanol was added to the filtrate to make up a volume of 10 ml. Then, the filtered extract was poured into a cuvette and put it into a Shimadzu UV2550 spectrophotometer to measure the absorbances at 665 nm at E665 and 750 nm at E750. After that 1 mol/L of hydrochloric acid was added to the cuvette for acidification, covered, and shaken well, and finally, the absorbances after 1 min at A665 and A750 at 665 nm and 750 nm, respectively, were measured. The concentration of chlorophyll-a was calculated according to the absorbances.

Research Methods and Accuracy Evaluation

Accuracy Evaluation Index

The atmospheric-correction and water-quality parameter retrieval use the mean relative error (MRE) and RMSE for accuracy evaluation:

$$MRE = \frac{1}{n} \sum_{1}^{n} \frac{|R_i - R_j|}{R_j} \times 100\% \tag{2}$$

$$RMSE = \sqrt{\frac{\sum_{1}^{n} (R_i - R_j)^2}{n}} \tag{3}$$

The standard deviation (SD) of the dispersion of statistical values of the water-quality retrieval results can be calculated as follows:

$$SD = \sqrt{\frac{1}{K} \sum_{a=1}^{K} (x_a - \mu)^2} \tag{4}$$

In Eqs. (2–4), n represents the number of points, R_i represents the value of water-quality parameter after retrieval or atmospheric-corrected reflectance value, and R_j represents the actual measurement. The water-quality parameter or measured equivalent spectral reflectance value, K, represents the number of samples, x_a represents the a-th sample, and μ represents the average value of the samples.
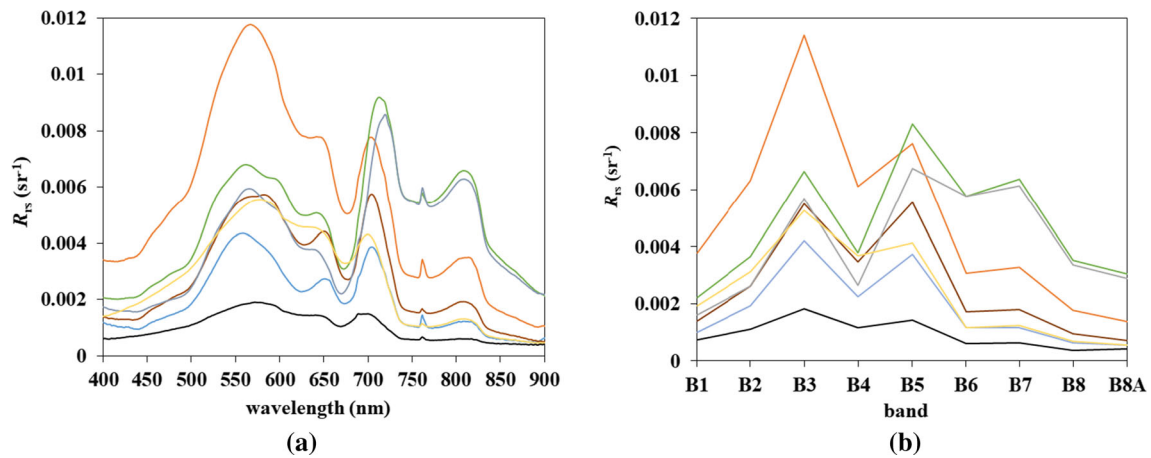
Fig. 2 **a** Measured spectral reflectance of surface water and **b** the equivalent spectral reflectance of Sentinel-2 in Xiong'an New Area on 5 October 2018

Evaluation of Atmospheric Correction and Effect

To quickly perform atmospheric correction on the Sentinel-2 data, the ESA released a plug-in, Sen2cor, which specialises in the production of L2A-level data. Sen2cor can perform atmospheric correction on Sentinel 2A/2B to obtain L2A-level data and was used in this study. To ensure the accuracy of the atmospheric-correction results, the spectral reflectance of each water sample after equivalence is fitted to the remote-sensing reflectance of Sentinel-2 satellite image after atmospheric correction. The reflectance of each band after fitting is shown in Fig. 3.

The measured spectral reflectance of seven waterbodies collected in the Xiong'an New Area on 5 October 2018 and the atmospheric correction of the remote-sensing reflectance of the image were subjected to corresponding regression analysis. To analyse the accuracy of Sen2cor atmospheric correction, the measured spectral reflectance of the waterbody and the results of atmospheric correction were used to extract the remote-sensing reflectance in the Band2–Band8A range for regression analysis. The results

are shown in Fig. 4. Figure 4 shows that the results obtained by Sen2cor have a high correlation with the measured values, and the data are more concentrated overall. When the reflectivity is 0.004–0.008 sr^{-1}, the data obtained are relatively discrete. This may be because the error may be larger in the band with the largest rate of change in the spectral curve. The determination coefficient R^2 of the remote-sensing reflectance results obtained by the Sen2cor atmospheric-correction method is 0.85, the RMSE is 0.0011 sr^{-1}, and the average relative error is 29.51%.

Water-Extraction Method and Result Evaluation

The waterbody-extraction algorithm used in this study uses the newly proposed relative water index (RWI) (Wu et al. 2020), which is formulated as follows:

$$RWI = \frac{(R_{rs}(560) + R_{rs}(705)) - (R_{rs}(842) + R_{rs}(865) + R_{rs}(2190))}{R_{rs}(560) + R_{rs}(705) + R_{rs}(842) + R_{rs}(865) + R_{rs}(2190)}$$
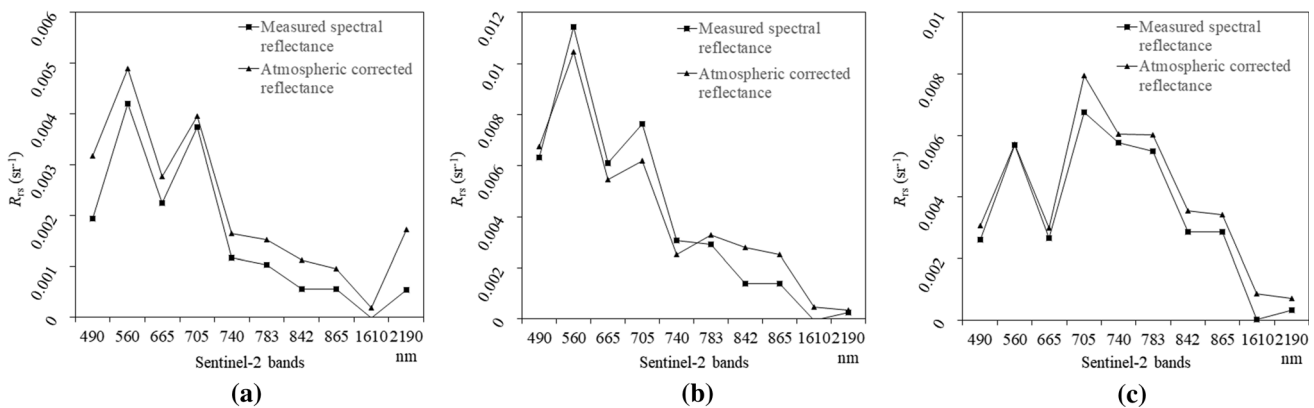
(5)

Fig. 3 Measured reflectance and atmospheric-corrected reflectance of samples **a** 1, **b** 2, and **c** 3 in Xiong'an New Area on 5 October 2018
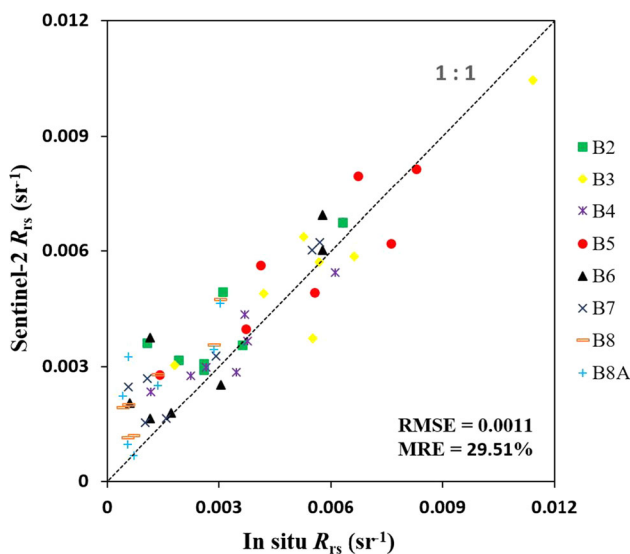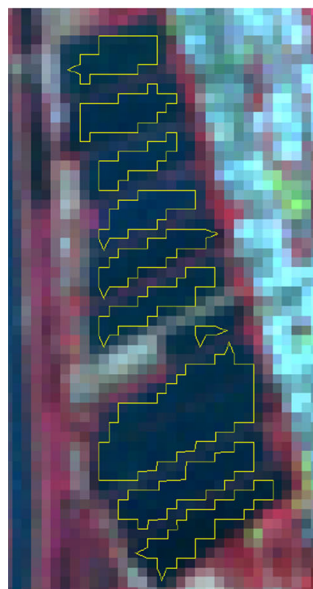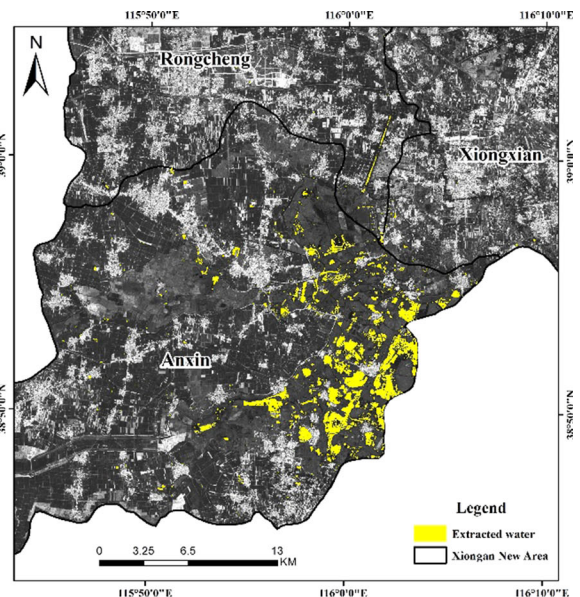
Fig. 4 B2–B8A band measured values and atmospheric-correction results reflectance regression analysis results

where R_{rs} (560), R_{rs} (705), R_{rs} (842), R_{rs} (865), and R_{rs} (2190) are the remote-sensing reflectance of Sentinel-2 bands 3, 5, 8, 8a, and 12, respectively. The waterbody boundary extracted by the RWI algorithm shows a better extraction effect than the other methods, and it can eliminate the influence of mountains and building shadows, cloud shadows, and mixed pixels to a certain extent. The water-boundary effect extracted by RWI is shown in Fig. 5a. The RWI was used to extract waterbodies from 35 time-phase mosaic images selected from 2016 to 2019, and each of the waterbodies differed with respect to area. This study was aimed at determining the temporal changes of

surface-water quality in the Xiong'an New Area and did not consider the changes in the area of the waterbodies. Therefore, the results of water extraction were intersected. This method can remove the influence of changes in the area of a waterbody and in the case where a part of the image, which could be a building shadow, is mistaken for a waterbody, such an error can be eliminated by obtaining the intersection of the water surface pixels. Finally, the waterbody with an unchanged area within Xiong'an New Area was obtained from 2016 to 2019. The waterbody-extraction results are shown in Fig. 5b.

Water-Quality Parameter Retrieval Algorithm and Accuracy Evaluation

Turbidity Retrieval Algorithm

In the near-infrared and visible light bands, the water turbidity increases along with the spectral reflectance. The turbidity level and spectral reflectance of the water have a linear correlation in the red band (Lin et al. 2004). In this study, blue, green, and red bands were selected for performing turbidity retrieval, and the measured data from May 2019 were used to construct a turbidity retrieval algorithm, which can be expressed as follows:

$$
T_{ntu} = 18182 \times \left(\frac{R_{rs}(560) \times R_{rs}(665)}{R_{rs}(490)} \right)^2 + 31763 \\
\times \left(\frac{R_{rs}(560) \times R_{rs}(665)}{R_{rs}(490)} \right) + 1.08 \tag{7}
$$

Fig. 5 a Water extraction boundary effect map and **b** water extraction result map

(a)

(b)

where $R_{rs}(490)$, $R_{rs}(560)$, and $R_{rs}(665)$ correspond to the blue, green, and red bands of the Sentinel data, respectively.

Chlorophyll-A Retrieval Algorithm

The absorption coefficient spectrum of chlorophyll-a in an inland waterbody mainly has two absorption peaks that are usually located near 440 and 675 nm. The peak at 440 nm is greatly affected by the absorption of non-pigmented suspended solids and yellow substances, while that at 675 nm is less affected by other water elements; therefore, the characteristic spectrum near 675 nm was selected in this study corresponding to the fifth band of the red edge band of Sentinel-2 data (Gilerson et al. 2010; Matthews 2011; Odermatt et al. 2012). The chlorophyll-a concentration retrieval algorithm was established using the measured data of 29 samples of Lake Baiyangdian in May 2019 as follows:

$$C_{chla} = 113.23 \times \left(\frac{R_{rs}(665)}{R_{rs}(705)}\right)^2 - 311.67 \times \left(\frac{R_{rs}(665)}{R_{rs}(705)}\right) + 216.76$$

(8)

where C_{chla} represents the retrieved chlorophyll-a concentration [µg/L], and $R_{rs}(665)$ and $R_{rs}(705)$ represent the red bands of the Sentinel-2 data and the fifth band, respectively.

Accuracy of Results of the Water-Quality Parameter Retrieval Algorithm

To ensure the reliabilities of remote-sensing monitoring and retrieval algorithms, the measured turbidity and chlorophyll-a concentration of the seven water samples in the Xiong'an New Area obtained on 5th October 2018 were regressed. In addition, the turbidity and chlorophyll-a concentration values obtained through the retrieval showed a significant correlation between the two sets of data. When the correlation coefficient between the measured and retrieved turbidity values of the waterbody reached 0.89, the MRE and RMSE were 23.31% and 3.18 NTU, respectively. When the correlation coefficient between the measured and retrieved chlorophyll-a concentrations in the waterbody reached 0.96, the MRE and RMSE were 31.23% and 9.09 µg/L, respectively. The results are shown in Fig. 6.

Results

Owing to the large area of the Xiong'an New Area and the small surface waterbodies, it is difficult to show the surface water of the entire district as most of the water is distributed in the Baiyangdian area of Anxin County. The area with a larger number and density of waterbodies in the inner Lake Baiyangdian is used as the display range.

According to the results of the time-series analysis of turbidity retrieval of surface water in Xiong'an New Area from 2016 to 2019 (Fig. 7) and statistics (Fig. 8), the turbidity of surface water was higher in 2016 and spring of 2017. After that, a significant drop was observed. In addition, from April 2016 to September 2019, the turbidity gradually declined with slight fluctuations during autumn 2016 and spring 2017. The seasonal-average highest and lowest values of turbidity were 40 NTU and 8.3 NTU in spring of 2016 and 2019, respectively. The four-year average value of turbidity was 22 NTU, and the SD was 9.5 NTU. No obvious change rule for turbidity in space existed, and the distributions of high and low turbidity were relatively uniform.

The time-series results of chlorophyll-a concentration retrieval in the surface water of the Xiong'an New Area from 2016 to 2019 (Fig. 8) and the statistical chart (Fig. 9) show that the chlorophyll-a concentration is low in spring and high in summer, followed by autumn. The chlorophyll-a concentration in the waterbody generally showed a weak downward trend with a low value in spring and a high value in summer. The four-year average was 31.3 µg/L, and the SD was 2.5 µg/L. No obvious change pattern for chlorophyll-a concentration in space was observed, and the distributions of high and low values of chlorophyll-a concentration were relatively uniform.

Discussion

Analysis of Impact of Policies on Surface-Water Quality in the Xiong'an New Area

The mean values of the chlorophyll-a concentration and turbidity of the whole image were calculated for each date selected in this study and plotted as a change curve as shown in Fig. 10. The figure shows that since the establishment of the Xiong'an New Area, the environmental governance work has been fruitful.

Earlier, many industries such as paper, leather, shoe-making, printing and dyeing, rubber, down and feather, and workshops existed in the upper reaches of Lake Baiyangdian with high levels of water consumption, energy consumption, pollution and sewage discharge along with rural
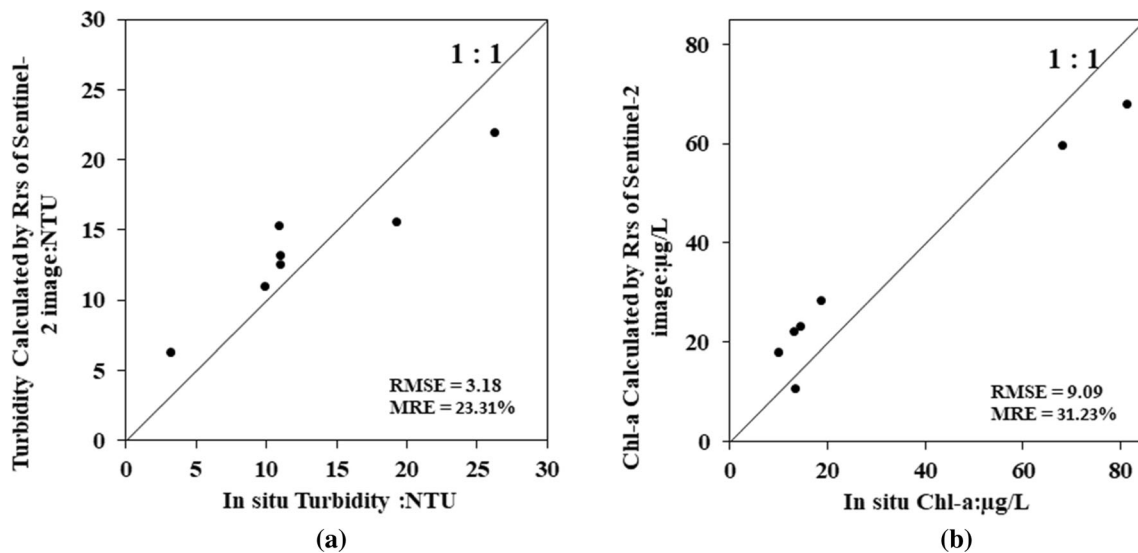
Fig. 6 Scatterplots of the comparison between the retrieval and measured values of turbidity and chlorophyll-*a* concentration. **a** Regression analysis of the retrieved and measured turbidities and **b** regression analysis of the retrieved and measured chlorophyll-*a* concentration

sewage discharge and garbage accumulation along the river. With the economic development of the villages along the river, the unreasonable use of pesticides and chemical fertilisers required by the planting industry and the accumulation of bait and animal faeces from the breeding industry increased the agricultural non-point source of pollution to the nearby rivers. Increase in population led to an increase in cultivation area in the region causing large-scale reclamation of cultivated land leading to water loss, shallow river siltation, soil fertility decline, and poor surface-water quality. Since 1958, many large- and medium-sized reservoirs were built in the upper reaches of Lake Baiyangdian. Due to the impoundment of reservoirs, many rivers have lost their natural water supply sources and are in a state of disconnection. The imbalance between economic and social development and water resources in the basin has led to the pollution of Lake Baiyangdian. After 2002, The Lake Baiyangdian Natural Wetland Reserve has become a tourist attraction again. The development of tourism has driven the surrounding industries. However, due to the lack of relevant laws and regulations and a standard system of ecological environment protection, the pollution caused by tourism is increased gradually.

Since the establishment of the Xiong'an New Area, the government has taken a series of measures including shutting down or rectifying large-scale high-pollution and high-emission enterprises, strengthening the treatment of domestic sewage and garbage, and improving farming methods in and around the lake region, thereby promoting green and pollution-free agriculture, reducing the use of pesticides and fertilisers and pollutant emissions, and saving water resources. Designated breeding areas, optimised breeding mode, and the removal of cages, net fences,

and net enclosures, earthwork and enclosure cleanup, scientific planning and management, and control on the scale and capacity of breeding have been implemented. Furthermore, sediment dredging, dismantling of water-intensive projects, and increasing the amount of water inflow into the Lake Baiyangdian have been implemented. Additionally, water-saving measures such as rational use of reclaimed water to prevent water diversion outside the river and interception of groundwater along the river have been implemented. These comprehensive measures from May to June 2017 have caused a significant decrease in turbidity in the surface waterbodies (Fig. 10), indicating that the Chinese government has achieved remarkable results in water treatment and conservation in the region.

Characteristics of Chlorophyll-a Concentration Changes

Figure 8 shows that the chlorophyll-*a* concentration in the Xiong'an New District during 2016–2019 is low in spring and high in summer and autumn. To understand this pattern, the authors collected historical weather data of the region through a weather-based website (http://tianqi.2345.com/wea_history/ 72,105.htm) and found that the temperature in the district was lower during spring and higher in summer and autumn. The warm-water environment can effectively promote the growth of phytoplankton and produce chlorophyll-*a* concentrations that are lower in spring and higher in summer and autumn. Therefore, chlorophyll-*a* concentration is proportional to the temperature in the district.

Through repeated field observations and using images in May 2019, the growth of diverse types of water plants was
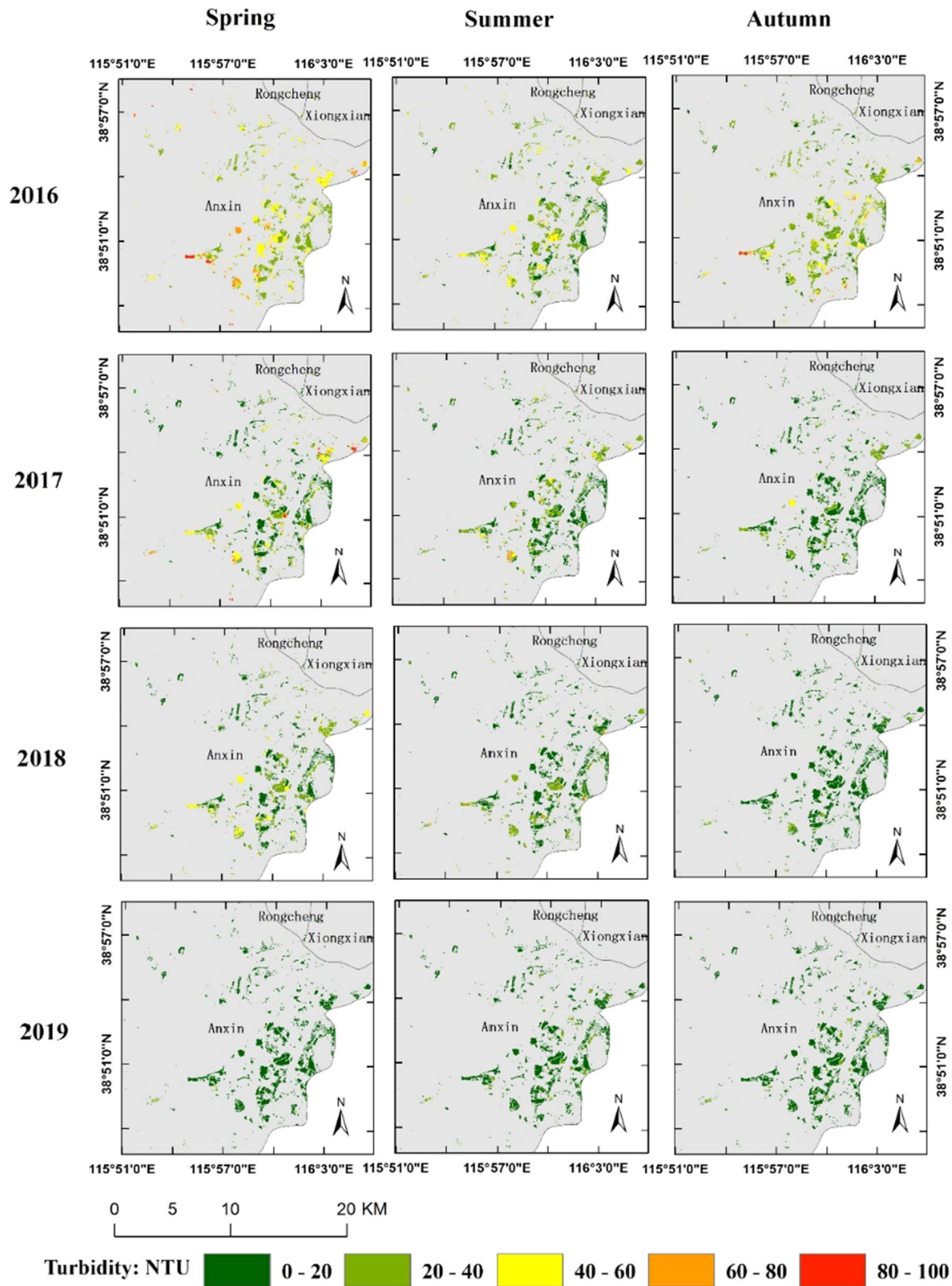
Fig. 7 Graphical representation of the temporal change of surface-water turbidity in Xiong'an New Area from 2016 to 2019

observed on the surface of the waterbody in Lake Baiyangdian Area as shown in Fig. 11. Figure 11a and c shows two kinds of floating-leaf water plants that are removed when the waterbody is extracted. The water grass in Fig. 11e grows underwater. When the water is extracted, it may be mistakenly divided into waterbodies. The growth

Fig. 8 Statistics of time-series changes of surface-water turbidity and chlorophyll-*a* concentration in Xiong'an New Area from 2016 to 2019
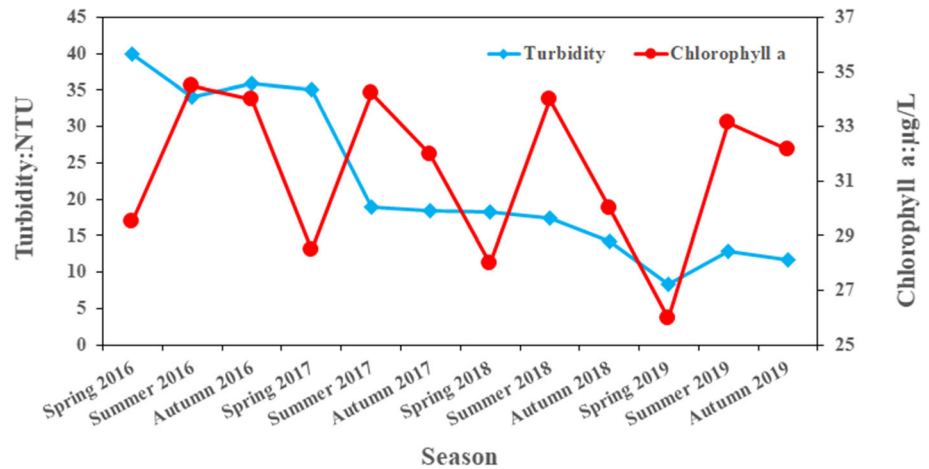
Characteristics of Water-Quality Changes in Partial Waterbodies

The sizes of the selected waterbodies are shown in Fig. 12. In addition, Fig. 13 shows the changes in the chlorophyll-*a* concentration and turbidity in the two areas. As shown in Fig. 13, the local waterbodies in the region show a declining trend in turbidity from 2016 to 2019. The chlorophyll-*a* concentration also fluctuates, i.e. it is low in spring and high in summer and autumn in the waterbodies outside the Lake Baiyangdian area. During 2016–2019, the turbidity shows an overall downward trend; however, this trend is not obvious. The change in chlorophyll-*a* concentration is relatively gentle with an overall downward trend showing a low concentration because although the waterbody in the lake is divided into small sections, the water channels are connected and thus can be regarded as a single unit. Therefore, the trends in the quality of the waterbody (Lake Baiyangdian) and the overall quality of all the surface waterbodies in the Xiong'an New Area are the same. The waterbody outside the Lake Baiyangdian area is an independent pond. Water quality fluctuations are highly susceptible to environmental influences. Therefore, although turbidity fluctuates, no obvious downward trend is observed. Moreover, because the algae content in the pond is relatively stable, it is not strongly affected by weather. Therefore, the content of chlorophyll-*a* during 2016–2019 is relatively stable, and the change is not obvious.

of underwater plants will influence the concentration of chlorophyll-*a*, and the growth of water grass is affected by seasonal changes that are more significant in summer and autumn. Therefore, the change in chlorophyll-*a* concentration in the surface water of the region is affected by air temperature and submerged water plants.

Comparison with Other Researches

The main advantages of this article are as follows. (1) The article analyses the surface water quality of Xiong'an New Area in time series based on remote-sensing data and not only analyses the reasons for the change of Lake Baiyangdian water body area (Liu et al. 2006; Li et al. 2017a, b; Wang et al. 2018; Song et al. 2018). (2) The retrieval algorithm for chlorophyll-*a* and turbidity suitable for Xiong'an New Area was constructed. The article compares the chlorophyll-*a* and turbidity retrieval algorithms proposed by other scholars in recent years and verifies the retrieval accuracy of each method based on the R_{rs} of Sentinel-2 image, as shown in Table 2 and 3. It can be seen from the table that the chlorophyll-*a* and turbidity retrieval algorithm proposed in this paper has higher accuracy. According to the retrieval results of chlorophyll-*a* in this article, we calculated the nutrient index TSI (Carlson. 1977). The results of TSI show that most surface water bodies in Xiong'an New Area have serious eutrophication. The chlorophyll-*a* and turbidity retrieval algorithms proposed in the article have good applicability to this type of water bodies and can provide a certain reference basis for subsequent researchers.

Conclusion

The surface waterbodies in the Xiong'an New Area were chosen for research as this region acts as the fulcrum for easing the non-capital administrative functions of Beijing, the capital of China, and plays a vital role in the coordinated development of the Beijing–Tianjin–Hebei economic belt, which is currently the national focus. Multispectral Sentinel-2 data, field experiments, and spectral data of the surface waterbodies of the Xiong'an New Area, and various water-quality parameters were used to analyse the
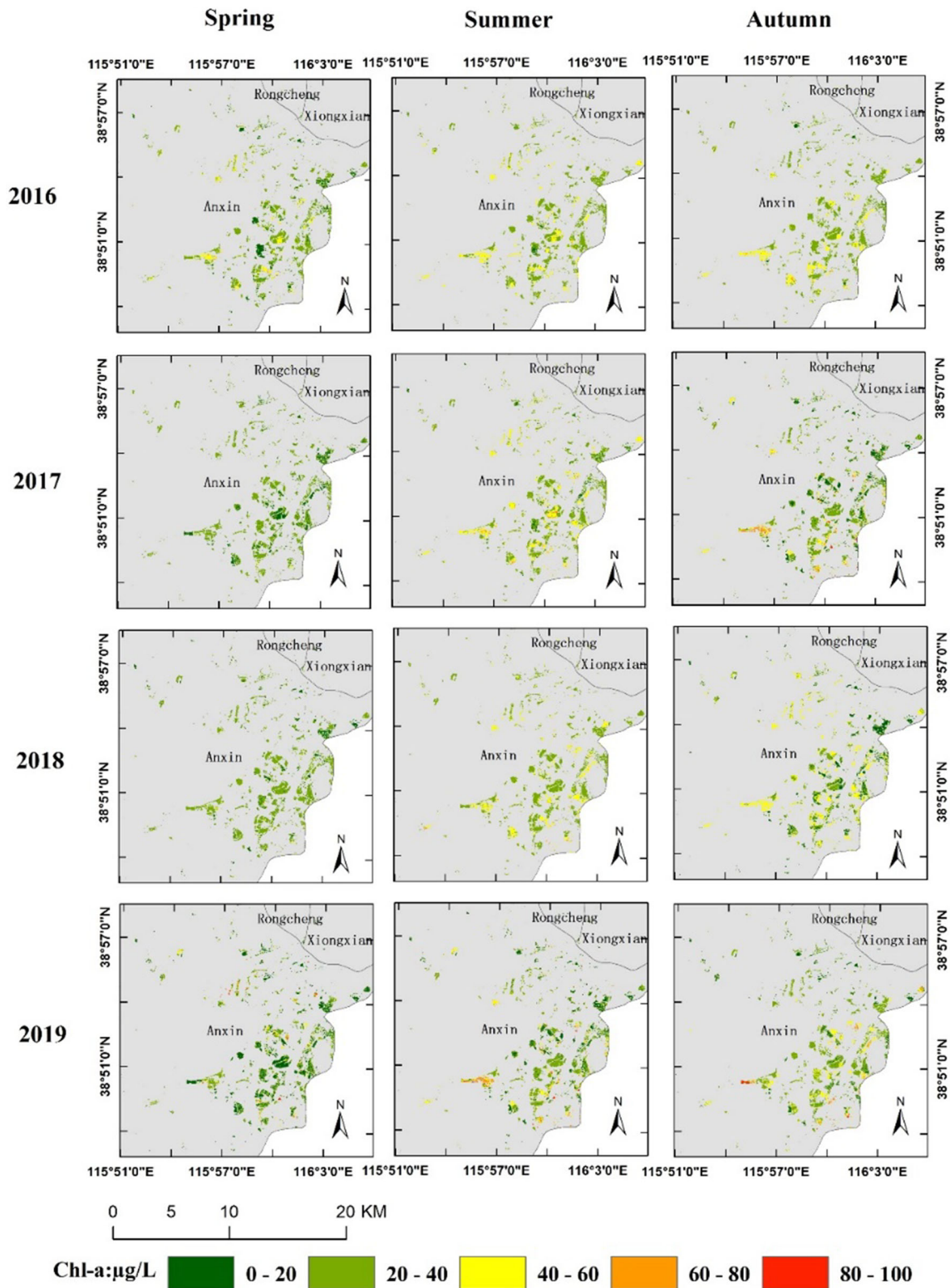
Fig. 9 Results of chronological changes in the chlorophyll-*a* concentration in the surface water of Xiong'an New Area from 2016 to 2019

chlorophyll-*a* concentration and turbidity for the period 2016 to 2019. The following conclusions can be drawn from this study. (1) The turbidity of the surface water in the

Xiong'an New Area declined gradually from April 2016 to September 2019 with the decrease clearly evident after the spring of 2017. The seasonal-average highest value of
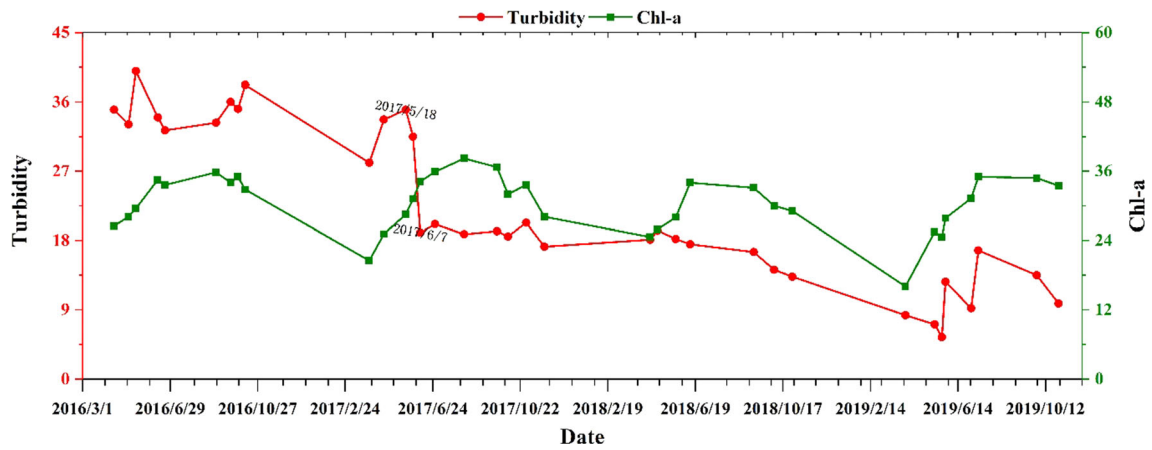
Fig. 10 Diurnal changes in the turbidity and chlorophyll-*a* concentration (Chl-*a*) of surface-water bodies in Xiong'an New Area from 2016 to 2019

Fig. 11 a and **c** Two kinds of floating water plants, the corresponding video images of which in **b** and **d** were captured using Sentinel-2 satellites. **e** Submerged water plants and **f** their corresponding satellite-captured image
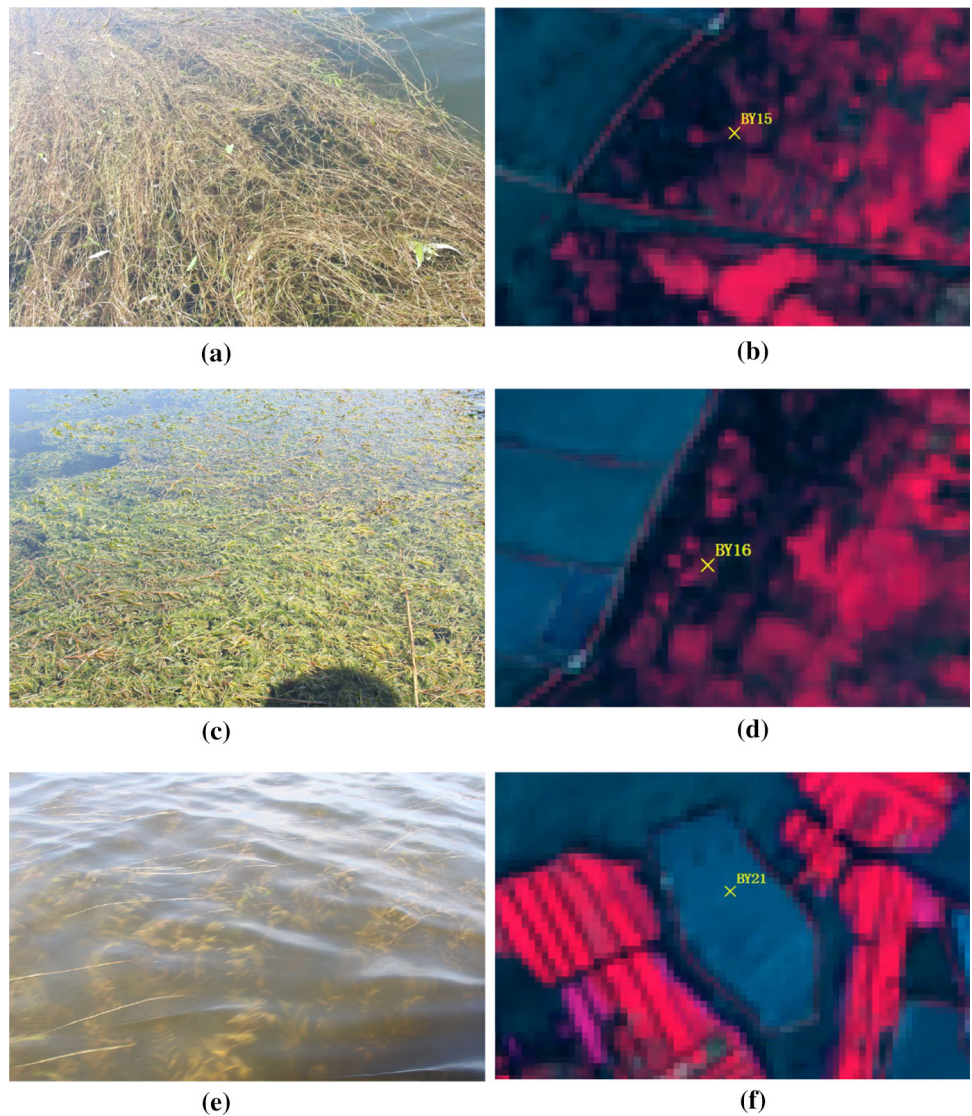
Fig. 12 Local water bodies inside and outside Lake Baiyangdian in Xiong'an New Area. **a** Inner and **b** outer parts of the water body in Baiyangdian are represented by yellow boxes

(a)

(b)

(a)

(b)

(c)

(d)
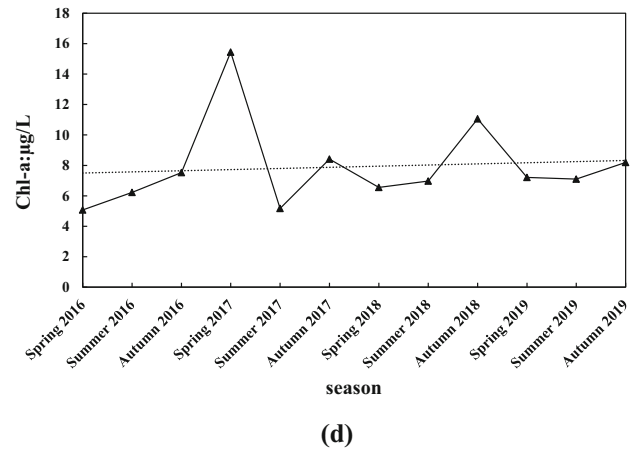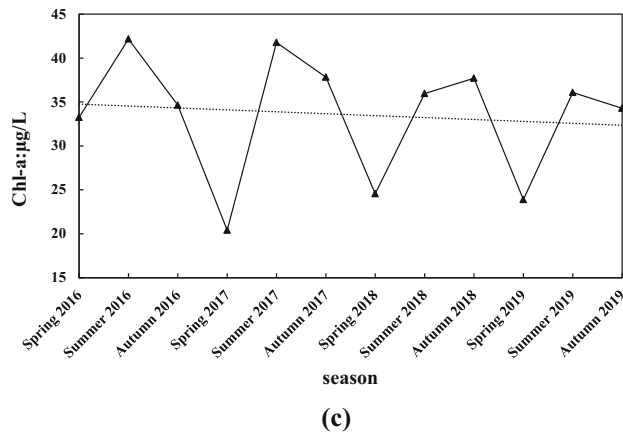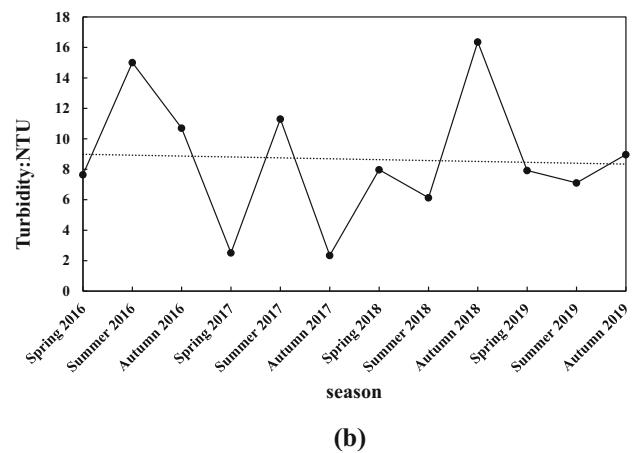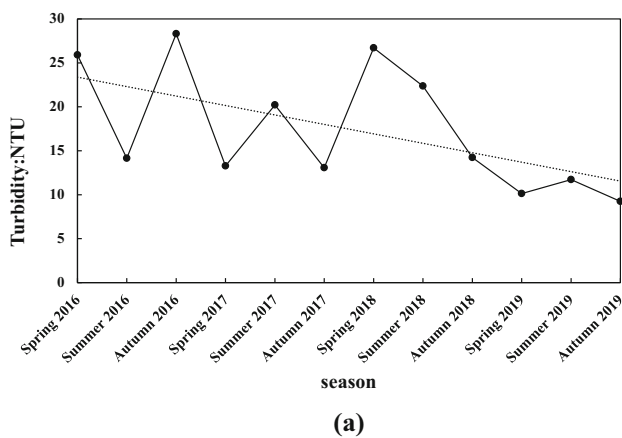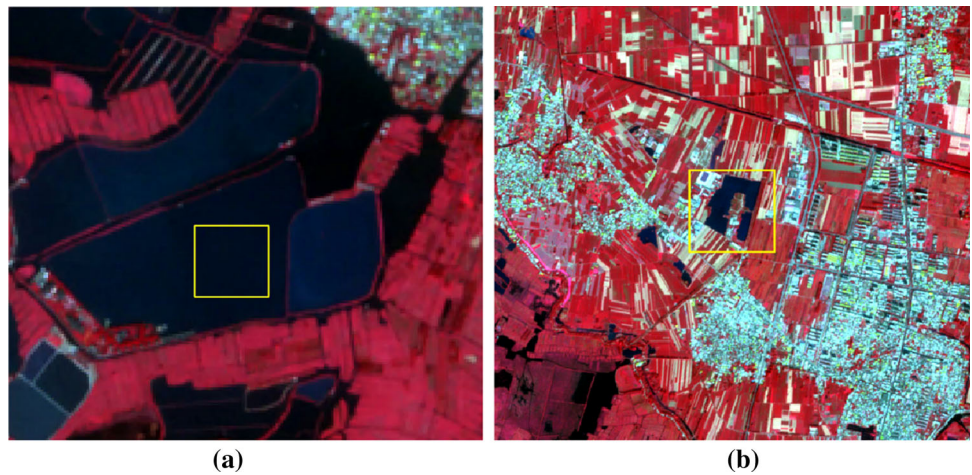
Fig. 13 Statistics of water-quality changes in local water bodies inside and outside Lake Baiyangdian from 2016 to 2019. **a** Statistical result of turbidity in Fig. 12a. **b** Statistical result of turbidity in Fig. 12b. **c** Statistical results of chlorophyll-*a* concentrations in Fig. 12a. **d** Statistical results of chlorophyll-*a* concentrations in Fig. 12b

turbidity was 40 NTU in the spring of 2016, and the lowest value was 8.3 NTU in the spring of 2019. The four-year average value of turbidity was 22 NTU and the SD was 9.5 NTU. (2) The concentration of chlorophyll-*a* in the surface waterbody of the Xiong'an New Area was lower in spring and higher in summer and autumn. This concentration generally showed a weak downward trend, with low and high values in spring and summer, respectively. The

Table 2 Performance of different Chla retrieval algorithms, where the coefficients were recalibrated using the field-measured spectra and Chla datasets of the current study

Model	Equation form	Satellite-based	
		MRE(%)	RMSE(μg/L)
Smith et al. (2018)	$y = (35.75 * RE/R - 19.3)^{1.124}$	43.61	18.41
Neil et al. (2019)	$y = 16.409 * (RE/R)^{2.1313}$	40.29	15.87
Lien et al. (2020)	$y = -11.64 * ((N - G)/(N + G)) - 26.89 * ((N - G)/(N + G)) + 8.01$	65.31	26.1
This study	$y = 113.23 * (R/RE)^2 - 311.67 * (R/RE) + 216.76$	31.23	9.09

Accuracy matrices for Chla estimates using satellite R_{rs} are listed in the table. $G = R_{rs}(560)$, $R = R_{rs}(665)$, $RE = R_{rs}(705)$, $N = R_{rs}(842)$

Table 3 Performance of different turbidity retrieval algorithms, where the coefficients were recalibrated using the field-measured spectra and turbidity datasets of the current study

Model	Equation form	Satellite-based	
		MRE(%)	RMSE(NTU)
Joshi et al. (2017)	$y = 6568.23 * R^{1.95}$	52.11	9.57
Liu and Wang (2019)	$y = -74.26 * B - 14.84 * G + 267.45 * R - 126.89 * N + 4.21$	37.59	5.24
Abirhire et al.(2020)	$y = -1.3790 + 55.3844 * N + 6.4725 * R/G - 5.6511 * N/G$	39.18	7.66
This study	$y = 18,182 * (G * R/B)^2 + 31,763 * (G * R/B) + 1.08$	23.31	3.18

Accuracy matrices for turbidity estimates using satellite R_{rs} are listed in the table. $B = R_{rs}(490)$, $G = R_{rs}(560)$, $R = R_{rs}(665)$, $RE = R_{rs}(705)$, $N = R_{rs}(842)$

average concentration over the four years was 31.3 μg/L, and the SD was 2.5 μg/L. (3) A comparison of the variation characteristics of different parameters of the waterbodies in time series in the region for the period 2016 to 2019 shows similar local and overall trends. The changes in water-quality parameters outside the Lake Baiyangdian region are not obvious. (4) Based on the turbidity and chlorophyll-a concentrations from 2016 to 2019, the water quality in this area shows an overall improvement, which is in line with the mitigating measures of the Chinese government for the region.

This paper provides a feasible theoretical basis for the inversion of surface water quality parameters in areas similar to Xiong'an New Area and will serve as a reference for other researchers to carry out similar monitoring studies. We provide a reasonable scheme to analyse water quality of relatively small surface water areas and facilitate effective technical support to and environmental management of small watersheds and discontinuous water areas through scientific decision-making. Furthermore, our approach can be used to improve the management of urban water environments and conduct quality-based classification of small surface water bodies in China and other parts of the world.

Compliance with ethical standards

References

Abirhire, O., Davies, J.-M., Guo, X., & Hudson, J. (2020). Understanding the factors associated with long-term reconstructed turbidity in Lake Diefenbaker from Landsat-imagery. *Science of the Total Environment, 724,* 138222. https://doi.org/10.1016/j.scitotenv.2020.138222.

Brezonik, P., Menken, K. D., & Bauer, M. (2005). Landsat-based remote sensing of lake water quality characteristics, including chlorophyll and colored dissolved organic matter (CDOM). *Lake and Reservoir Management, 21*(4), 373–382. https://doi.org/10.1080/07438140509354442.

Caballero, I., Navarro, G., & Ruiz, J. (2018). Multi-platform assessment of turbidity plumes during dredging operations in a major estuarine system. *International Journal of Applied Earth Observation and Geoinformation, 68,* 31–41. https://doi.org/10.1016/j.jag.2018.01.014.

Carlson, R. E. (1977). A trophic state index for lakes. *Limnology and Oceanography, 22*(2), 361–369.

Chen, J., Zhu, W., Tian, Y. Q., Yu, Q., Zheng, Y., & Huang, L. (2017). Remote estimation of colored dissolved organic matter and chlorophyll-a in Lake Huron using Sentinel-2 measurements. *Journal of Applied Remote Sensing*. https://doi.org/10.1117/1.JRS.11.036007.

Chowdhury, R. A., Rashid, T., & Hoque, S. (2014). Assessing surface water quality using landsat TM and in situ data: An exploratory analysis. In A. Dewan & R. Corner (Eds.), *Dhaka Megacity Springer Geography*. Dordrecht: Springer.

Drusch, M., Del Bello, U., Carlier, S., Colin, O., Fernandez, V., Gascon, F., et al. (2012). Sentinel-2: ESA's optical high-resolution mission for GMES operational services. *Remote Sensing of Environment, 120,* 25–36. https://doi.org/10.1016/j.rse.2011.11.026.

Gilerson, A. A., Gitelson, A. A., Zhou, J., Gurlin, D., Moses, W., Ioannou, I., et al. (2010). Algorithms for remote estimation of chlorophyll-a in coastal and inland waters using red and near infrared bands. *Optics Express, 18*(23), 24109–24125. https://doi.org/10.1364/OE.18.024109.

Huovinen, P., Ramírez, J., Caputo, L., & Gómez, I. (2019). Mapping of spatial and temporal variation of water characteristics through satellite remote sensing in Lake Panguipulli, Chile. *Science of the Total Environment, 679,* 196–208. https://doi.org/10.1016/j.scitotenv.2019.04.367.

Joshi, I. D., D'Sa, E. J., Osburn, C. L., & Bianchi, T. S. (2017). Turbidity in Apalachicola Bay, Florida from landsat 5 TM and field data: Seasonal patterns and response to extreme events. *Remote Sensing, 9*(4), 367. https://doi.org/10.3390/rs9040367.

Kuhn, C., de Matos Valerio, A., Ward, N., Loken, L., Sawakuchi, H. O., Kampel, M., et al. (2019). Performance of Landsat-8 and Sentinel-2 surface reflectance products for river remote sensing retrievals of chlorophyll-a and turbidity. *Remote Sensing of Environment, 224,* 104–118. https://doi.org/10.1016/j.rse.2019.01.023.

Kutser, T., Paavel, B., Verpoorter, C., Ligi, M., Soomets, T., Toming, K., et al. (2016). Remote sensing of black lakes and using 810 nm reflectance peak for retrieving water quality parameters of optically complex waters. *Remote Sensing, 8*(6), 497. https://doi.org/10.3390/rs8060497.

Lambin, E., & Strahlers, A. (1994). Change-vector analysis in multitemporal space: A tool to detect and categorize land-cover change processes using high temporal-resolution satellite data. *Remote Sensing of Environment, 48*(2), 231–244. https://doi.org/10.1016/0034-4257(94)90144-9.

Li, C., Zheng, X., Zhao, F., Wang, X., Cai, Y., & Zhang, N. (2017). Effects of Urban Non-Point source pollution from Baoding City on Baiyangdian Lake China. *Water, 9*(4), 249. https://doi.org/10.3390/w9040249.

Li, T., Tian, L., Li, J., Zhang, L., & Sun, Z. (2017). Comparative study on chlorophyll retrieval of turbid water based on Sentinel satellite—Taking Poyang lake as an example. *Journal of Huazhong Normal University (Natural Science Edition), 51*(6), 858–864.

Lien, R.-L., Iongel, D.-L., Lisdelys, G.-R., Rodrigo, A.-e-R., Rolando, C., Oscar, P., et al. (2020). Spectral analysis using LANDSAT images to monitor the chlorophyll-a concentration in Lake Laja in Chile. *Ecological Informatics*. https://doi.org/10.1016/j.ecoinf.2020.101183.

Lin, G., Fang, J., & Chen, F. (2004). Remote sensing analysis on the evolution trend of beach and trough in Tongan Bay, Xiamen. *Remote Sensing for Land and Resources, 4,* 63–67.

Liu, C., Xie, G., & Huang, H. (2006). Shrinking and drying up of Baiyangdian Lake wetland: A natural or human cause? *Chinese Geographical Science, 16*(4), 314–319. https://doi.org/10.1007/s11769-006-0314-9.

Liu, H., Li, Q., Shi, T., Hu, S., Wu, G., & Zhou, Q. (2017). Application of sentinel 2 MSI images to retrieve suspended particulate matter concentrations in Poyang Lake. *Remote Sensing, 9*(7), 761. https://doi.org/10.3390/rs9070761.

Liu, L., & Wang, Y. (2019). Modelling reservoir turbidity using landsat 8 satellite imagery by gene expression programming. *Water, 11*(7), 1479. https://doi.org/10.3390/w11071479.

Matthews, M. W. (2011). A current review of empirical procedures of remote sensing in inland and near-coastal transitional waters. *International Journal of Remote Sensing, 32*(21), 6855–6899. https://doi.org/10.1080/01431161.2010.512947.

Mueller, J. L. (2003). Ocean optics protocols for satellite ocean colour sensor validation, revision 4, volume III: Radiometric measurements and data analysis protocols. *National Aeronautical and Space Administration Report, 21621,* 1–72. https://doi.org/10.1002/bjs.18004720152.

Neil, C., Spyrakos, E., Hunter, P. D., & Tyler, A. N. (2019). A global approach for chlorophyll-a retrieval across optically complex inland waters based on optical water types. *Remote Sensing of Environment, 229,* 159–178. https://doi.org/10.1016/j.rse.2019.04.027.

Odermatt, D., Gitelson, A., Brando, V. E., & Schaepman, M. (2012). Review of constituent retrieval in optically deep and complex waters from satellite imagery. *Remote Sensing of Environment, 118,* 116–126. https://doi.org/10.1016/j.rse.2011.11.013.

Rostami, S., He, J., & Hassan, Q. (2018). Riverine water quality response to precipitation and its change. *Environments, 5*(1), 8. https://doi.org/10.3390/environments5010008.

Smith, M. E., Robertson Lain, L., & Bernard, S. (2018). An optimized chlorophyll a switching algorithm for MERIS and OLCI in phytoplankton-dominated waters. *Remote Sensing of Environment, 215,* 217–227. https://doi.org/10.1016/j.rse.2018.06.002.

Sola, I., García-Martín, A., Sandonís-Pozo, L., Álvarez-Mozos, J., Pérez-Cabello, F., González-Audícana, M., et al. (2018). Assessment of atmospheric correction methods for Sentinel-2 images in Mediterranean landscapes. *International Journal of Applied Earth Observation and Geoinformation, 73,* 63–76. https://doi.org/10.1016/j.jag.2018.05.020.

Song, C., Ke, L., Pan, H., Zhan, S., & Ma, R. (2018). Long-term surface water changes and driving cause in Xiong'an, China: From dense Landsat time series images and synthetic analysis. *Science Bulletin, 63*(11), 708–716. https://doi.org/10.1016/j.scib.2018.05.002.

Su, L., Liu, J., & Christensen, P. (2011). Spatial distribution and ecological risk assessment of metals in sediments of Baiyangdian wetland ecosystem. *Ecotoxicology, 20*(5), 1107–1116. https://doi.org/10.1007/s10646-011-0616-2.

Tang, J. W., Tiang, G. L., Wang, X. Y., Wang, X. M., & Song, Q. J. (2004). The methods of water spectral measurement and analysis I: Above water method. *Journal of Remote Sensing, 8*(1), 37–44.

TomingKutserLaasSeppPaavelNõges, K. T. A. M. B. T. (2016). First experiences in mapping lake water quality parameters with Sentinel-2 MSI imagery. *Remote Sensing, 8*(8), 640. https://doi.org/10.3390/rs8080640.

Vanhellemont, Q. (2019). Adaptation of the dark spectrum fitting atmospheric correction for aquatic applications of the Landsat and Sentinel-2 archives. *Remote Sensing of Environment, 225,* 175–192. https://doi.org/10.1016/j.rse.2019.03.010.

Vincent, R. K., Qin, X., McKay, R. M. L., Miner, J., Czajkowski, K., Savino, J., et al. (2004). Phycocyanin detection from LANDSAT TM data for mapping cyanobacterial blooms in Lake Erie. *Remote Sensing of Environment, 89*(3), 381–392. https://doi.org/10.1016/j.rse.2003.10.014.

Wang, X., Wang, W., Jiang, W., Jia, K., Rao, P., & Lv, J. (2018). Analysis of the dynamic changes of the Baiyangdian lake surface based on a complex water extraction method. *Water, 10*(11), 1616. https://doi.org/10.3390/w10111616.

Warren, M. A., Simis, S. G. H., Martinez-Vicente, V., Poser, K., Bresciani, M., Alikas, K., et al. (2019). Assessment of atmospheric correction algorithms for the sentinel-2A multi-spectral imager over coastal and inland waters. *Remote Sensing of Environment, 225,* 267–289. https://doi.org/10.1016/j.rse.2019.03.018.

Wei, M., Qiao, B., Zhao, J., & Zuo, X. (2020). The area extraction of winter wheat in mixed planting area based on Sentinel-2 a remote sensing satellite images. *International Journal of Parallel, Emergent and Distributed Systems, 35*(3), 297–308. https://doi.org/10.1080/17445760.2019.1597084.

Wu, Q. Wang, M., Shen, Q., Li, J., Zhang, F., Yao, Y. (2020). Research on small water body extraction method based on Sentinel-2 satellite multi-spectral remote sensing image. *Journal of Remote Sensing.* http://www.jors.cn/jrs/ch/reader/view_abstract.aspx?file_no=2 01909230000001&flag=2.

Xu, M., Liu, H., Beck, R., Lekki, J., Yang, B., Shu, S., et al. (2019). A spectral space partition guided ensemble method for retrieving chlorophyll-*a* concentration in inland waters from Sentinel-2A satellite imagery. *Journal of Great Lakes Research, 45*(3), 454–465. https://doi.org/10.1016/j.jglr.2018.09.002.

XuTianJaneLiDingCao, Q. F. M. B. Y. W. X., et al. (2012). Pollen source areas of lakes with inflowing rivers: Modern pollen influx data from Lake Baiyangdian, China. *Quaternary Science Reviews, 37,* 81–91. https://doi.org/10.1016/j.quascirev.2012.01.019.

Zhao, Y., Shen, Q., Wang, Q., Yang, F., Wang, S., Li, J., et al. (2020). Recognition of water colour anomaly by using Hue Angle and Sentinel 2 image. *Remote Sensing, 12*(4), 716. https://doi.org/10.3390/rs12040716.

Zhao, Y., Xia, X. H., Yang, Z. F., & Wang, F. (2012). Assessment of water quality in Baiyangdian Lake using multivariate statistical techniques. *Procedia Environmental Sciences, 13,* 1213–1226. https://doi.org/10.1016/j.proenv.2012.01.115.

Zhu, J., Zhou, Y., Wang, S., Wang, L., Liu, W., Li, H., et al. (2019). Analysis of the change of Baiyangdian wetland from 1975 to 2018. *Journal of Remote Sensing, 23*(5), 971–986. https://doi.org/10.11834/jrs.20198379.